ELSEVIER

ScienceDirect

Physics Procedia 2 (2009) 365–372

Physics Procedia

www.elsevier.com/locate/procedia

Excited state absorption spectroscopy of ZBLAN:Er^{3+} glass - experiment and simulation

D. Piatkowski[1*], K. Wisniewski[1,2], M. Rozanski[1], Cz. Koepke[1]

[1] Institute of Physics, Nicolaus Copernicus University, Grudziądzka 5/7, 87-100 Toruń, Poland

[2] Institute of Experimental Physics, University of Gdańsk, Wita Stwosza 57, 80-952 Gdańsk, Poland

[*]Corresponding author: dapi@fizyka.umk.pl

We present the excited state absorption (ESA) spectroscopy of ZBLAN:Er^{3+} glass. The experimental spectra were measured in broad spectral range (500–1800 nm) by the CW pump-probe technique. Judd–Ofelt (JO) approach was employed to interpret the results and to simulate the ESA spectra which were successfully confronted with the experiment. We also propose a systematic approach for prediction of various types of up-conversion mechanisms such as ESA up-conversion and photon avalanche (PA). Careful investigations were made to indicate possible up-conversion excitation channels in a wide spectral range, from 400 nm up to 2 μm.

PACS: 42.70.Hj; 32.70.Cs; 71.20.Eh; 31.50.+w
Keywords: Excited state absorption; Upconversion; Judd–Ofelt theory; Modelling and simulation

1. Introduction

The ESA measurement is one of the most complex spectroscopic experiment. It used to be performed just in few laboratories in the world, mostly in Europe. For decades the ESA experiment was addressed to development of new laser materials. And vice versa, improvement of the ESA experimental techniques was due to evolution of lasers. Among many rare-earths doped materials, neodymium [1, 2] and erbium [3, 4] doped ones were mostly explored as interesting media for lasers or telecommunication amplifiers. Therefore stimulated emission (SE) transitions and their spectral relationships with ESA transitions are of key importance. In this paper we present the ESA experiment as an excellent tool for investigation of new up-conversion excitation channels in widely known and popular ZBLAN:Er^{3+} glass. The composition of the glass was 53ZrF_4:20BaF_2:4LaF_3:3AlF_3:20NaF and it was activated by 2 mol% of ErF_3 substituted for LaF_3.

2. ESA experiment

Experimental setup bases on the CW pump-probe technique [5, 6] and was described in detail in our previous papers [7, 8]. The excitation beam was provided by an Ar^+ laser operating at 488 nm and utilizing $^4I_{15/2} \rightarrow {}^4F_{7/2}$ transition in the Er^{3+} ion. The probe and pump beams were modulated by mechanical choppers, TTI C-995, at frequencies 1 kHz and 10 Hz respectively. Overlap between the probe and pump beams was provided by a pinhole (0.5 mm) and perfectly centered optics (cage system, Thorlabs). As detectors served PIN photodiodes: Si (550–1000 nm) and InGaAs (1000–1800 nm) with direct anode current output, coupled to a 0.4 m prism monochromator. The resolution was 1 nm in the visible range and 2 nm in the NIR. Differences of the light intensities transmitted through the sample under laser excitation $\Delta I(\lambda)$, together with the probe intensity $I(\lambda)$, were measured simultaneously by a cascade of two DSP lock-in amplifiers (Signal Recovery 7265). The

doi:10.1016/j.phpro.2009.07.021

probe beam intensity was measured by the first lock-in (time constant 10 ms), where the high frequency chopper provided the reference. The output signal was accumulated by a computer and simultaneously analyzed by the second lock-in (time constant 5 s) where the difference intensity signal was measured. The final spectrum registered by a computer can be described by the approximated equation [9]

$$\frac{\Delta I(\lambda)}{I(\lambda)} = AL\left(N^* \sigma_{GSA}(\lambda) + \sum_i N_i^* \left(\sigma_{SE_i}(\lambda) - \sigma_{ESA_i}(\lambda) \right) \right) \tag{1}$$

which can be expressed as a superposition of σ_{GSA}, σ_{ESA} and σ_{SE} spectra, calculated with appropriate weights (populations densities), where A is the second lock-in amplification constant, L is the length of the sample, N^* is the total excited population density and N^*_i is population density in a particular i-th excited state. We call such a spectrum the excited state transmission (EST), to distinguish this form the pure ESA spectrum where $\sigma_{GSA} = \sigma_{SE} = 0$. Note that GSA and SE transitions are described by the same sign (+), in contrast with the ESA whose signal is negative. Experimental EST spectrum, measured in the range from 500 to 1800 nm, is shown in Fig.1a. It presents several ESA peaks competing with GSA and SE transitions. Possible up-conversion excitations will be discussed in chapter 4.

3. ESA calculations

The EST spectra can be calculated using a simple approach presented in our previous papers [7, 8]. Calculation are useful when one needs to recognize all the ESA transitions that appear in the experiment. Assuming that the complex GSA or ESA spectrum can be expressed as a linear superposition of the individual transitions peaks, we can use the expression

$$\sigma^{cal}(\nu) = \frac{e^2}{4\varepsilon_o m_e c^2} \sum_{i=1}^{N} f_i^{cal} G_i(\nu) \tag{2}$$

where G_i describes the profile of the absorption line, which can be approximated by the Gaussian in a glass matrix [10]. The oscillator strengths of the absorption transitions can be calculated using Judd–Ofelt approach [11, 12]. The intensity parameters calculated for ZBLAN:Er^{3+} system are following

$$\Omega_2 = (2.74 \pm 0.22) \times 10^{-20}\ \mathrm{cm}^2$$
$$\Omega_4 = (1.47 \pm 0.40) \times 10^{-20}\ \mathrm{cm}^2$$
$$\Omega_6 = (1.07 \pm 0.13) \times 10^{-20}\ \mathrm{cm}^2$$

and they are close to those found by other authors for similar systems [13, 14]. The intermediate coupling coefficients, necessary for the JO calculation, were found by diagonalization of the Hamiltonian of the free ion of Er^{3+} [15]. The energy parameters evaluated for ZBLAN:Er^{3+} system are presented in Tab.1 (RMS=37 cm^{-1}).

Apart of the oscillator strengths and energies of the transitions which can by simply calculated, line widths (Γ) which are necessary for spectra simulation, cannot be evaluated from the first principles. After Binnemans *et al.*, we treated Γ-s as parameters for the GSA spectra reproduction [16, 17]. Furthermore, we assumed that the same Γ values can be used for the ESA spectra simulation since GSA and ESA transitions lead to the same final states (see for example [7, 8]). The same procedure was used for simulation of the ESA spectra in the present paper. We calculated σ_{ESA} for the ESA transitions from two long-living states $^4I_{13/2}$

and $^4I_{11/2}$. To compare the simulated spectra with the experiment we have calculated the EST spectrum using Eq.(1) and the experimental σ_{GSA}, for the following weights

$$N^*(^4I_{13/2}) = 0.5\ N^* \text{ and } N^*(^4I_{11/2}) = 0.45\ N^*,$$

where the total excited population density have been evaluated as $N^* = 3.5\times10^{16}$ cm^{-3}.

The simulated EST spectrum is presented in the Fig.1b. We have obtained good agreement between the experiment and calculations. The ESA transition intensities as well as shape of the complex lines seem to be reconstructed correctly. Furthermore, we extrapolated the EST spectrum beyond the experimental range, up to 400 nm in the short wavelength part of the spectrum and 3 μm in the NIR.

4. Up-conversion excitation channels

Excited state absorption spectroscopy is an excellent tool for analysis of various types of the up-conversion mechanisms. Based on the EST spectra we can at once recognize candidates for the ESA-type or PA-type up-conversions. Look at the Fig.2 where theoretical EST spectrum is presented. When the ESA transition is separated from any other lines, we should consider such an excitation as a good candidate for the PA up-conversion (a). From theory of the PA mechanism it is known, that apart of intense ESA transition between two excited states $i \rightarrow f$, the efficient energy transfer feeding level i is also required [18]. Since we have no control of the energy transfer efficiency, energy of photons matching exactly the maxima of the ESA transition should be optimized based on the EST spectrum.

Another conversion mechanism seen in the EST spectrum is the ESA-type up-conversion. Sequential two-step absorption can be easy identified as GSA and ESA lines overlapping in some spectral range. Competing signals seen in the EST spectrum create a characteristic differential-like structure, presented in Fig.2 (b). Inflexion point should be considered as interesting for activation the ESA-type up-conversion, since the GSA and ESA transitions are of identical amplitude. Such investigations should be always connected with precise GSA spectra analysis.

Evaluated excitations wavelengths, potentially interested for activation of the ESA or PA-type up-conversion, are indicated by heavy dots in Fig.1. Exact assignment of the transitions involved along with proposed up-conversion mechanism are listed in Tab.2.

5. Conclusions

We have presented the excited state absorption spectroscopy of the ZBLAN:Er^{3+} glass. The EST spectrum has been measured in a wide spectral range from 500 to 1800 nm. The EST spectrum has been also simulated and successfully confronted with the experiment. We have proposed almost 20 excitation wavelengths which can be utilized to excite the anti-Stokes emissions in the ZBLAN:Er^{3+} system. Some of them are already known but most have not been verified until now.

Acknowledgment

Authors are very grateful to Professor Zygmunt Mierczyk, Military University of Technology, Warsaw, for supplying the samples. DP is grateful to Professor Mike Reid, University of Canterbury, Christchurch, New Zealand, for making possible to use his software. KW was supported by the Polish Committee for Scientific Research under project PBZ/MEiN/01/2006/39.

References

[1] S. Kück, L. Fornasiero, E. Mix, G. Hüber, Appl. Phys, B 67 (1998) 151.
[2] J.L. Doualan, C. Maunier, D. Descamps, J. Landais, R. Moncorgé, Phys. Rev. B 62 (2000) 4459.
[3] M. Pollnau, W. Lüthy, H.P. Weber, K. Krämer, H.U. Güdel, R.A. McFarlane, Appl. Phys. B 62 (1996) 339.
[4] C. Labbé, J.L. Doualan, S. Girard, P. Le Boulanger, J. Alloys Comp. 275–277 (1998) 264.
[5] T. Wegner, K. Petermann, Appl. Phys. B 49 (1989) 275.
[6] P. Le Boulanger, J.L. Doualan, S. Girard, J. Margerie, R. Moncorgé, Phys. Rev. B 60 (1999) 11380.
[7] D. Piątkowski , K. Wiśniewski, Cz. Koepke, M. Naftaly, Excited state absorption spectroscopy of Nd3+ activated fluoroaluminate glass – experiment and simulation, Opt. Mater. (2008) in press.
[8] D. Piątkowski, K. Wiśniewski, M. Różański, Cz. Koepke, M. Kaczkan, M. Klimczak, R. Piramidowicz, M. Malinowski, J. Phys.: Condens. Matter 20 (2008) 155201.
[9] J. Koetke, G. Hüber, Appl. Phys. B 61 (1995) 151.
[10] C. Görller-Walrand, K. Binnemans, Handbook on the physics and chemistry of rare earths, vol. 25, ch. 167, North-Holland, Amsterdam 1998.
[11] B.R. Judd, Phys. Rev. 127 (1962) 750.
[12] G.S. Ofelt, J. Chem. Phys. 37 (1962) 511.
[13] L. Wetenkamp, G.F. West, H. Többen, J. Non-Cryst. Solids 140 (1992) 35.
[14] M.D. Shinn, W.A. Sibley, M.G. Drexhage, R.N. Brown, Phys. Rev. B 27 (1983) 6635.
[15] B.G Wybourne, Spectroscopic properties of rare earths, John Wiley&Sons, Argonne, Illinois 1965.
[16] K. Binnemans, H. De Leebeeck, C. Görller-Walrand, J.L. Adam, Chem. Phys. Lett. 303 (1999) 76.
[17] D. Piątkowski, J. Non-cryst. Solids 353 (2007) 1017.
[18] M.-F. Joubert, Opt. Mater. 11 (1999) 181.
[19] R. Balda, J. Fernández, J.-L. Adam, L.M. Lacha, M.A. Arriandiaga, J. Non-Cryst. Solids 326-327 (2003) 330.
[20] F. Kaczmarek, Z. Stryła, A. Jendrzejczak, Appl. Phys. B 73 (2001) 125.
[21] M.J.V. Bell, D.F. de Sousa, L.A.O. Nunes, J.Appl. Phys. 87 (2000) 8264.
[22] L. Zhang, H. Hu, J. Non-Cryst. Solids 326–327 (2003) 353.
[23] Y. Chen, D. Meichenin, F. Auzel, J. Phys.: Condens. Matter 7 (1995) 3363.
[24] F. Auzel, Y. Chen, J. Lumin. 65 (1995) 45.
[25] S.R. Bullock, B.R. Reddy, P. Venkateswarlu, S.K. Nash-Stevenson, J.C. Fajardo, Opt. Quantum Electron. 29 (1997) 83.
[26] S. Ferber, V. Gaebler, H.J. Eichler, Opt. Mater. 20 (2002) 211.
[27] F. Auzel, Y. Chen, D. Meichenin, J. Lumin. 60–61 (1994) 692.

Tab.1. Free ion energy parameters evaluated for ZBLAN:Er^{3+} system.

Parameter (cm^{-1})		±
$\mathbf{E_{avg}}$	35811	13
$\mathbf{F^2}$	100314	118
$\mathbf{F^4}$	70678	297
$\mathbf{F^6}$	50108	201
$\boldsymbol{\zeta}$	2390	6
$\boldsymbol{\alpha}$	17.88	-
$\boldsymbol{\beta}$	-599	-
$\boldsymbol{\gamma}$	1719	-
$\mathbf{T^2}$	441	-
$\mathbf{T^3}$	42	-
$\mathbf{T^4}$	64	-
$\mathbf{T^6}$	-314	-
$\mathbf{T^7}$	387	-
$\mathbf{T^8}$	363	-
$\mathbf{P^2}$	852	-
$\mathbf{P^4}$	639	-
$\mathbf{P^6}$	426	-
$\mathbf{M^0}$	4.58	-
$\mathbf{M^2}$	2.57	-
$\mathbf{M^4}$	1.74	-

Tab.2. Evaluated excitation wavelengths considered as valid for activation ESA or PA-type of up-conversions.

Pump (nm)		Excitation channel		Mechanism	References
		1st step	2nd step		
A	1956	-	$^4I_{11/2} \rightarrow (^4F,^4I)_{9/2}$	PA	-
B	1704	-	$^4I_{13/2} \rightarrow {}^4I_{9/2}$	PA	-
C	1142	-	$^4I_{13/2} \rightarrow (^4F,^4I)_{9/2}$	PA	-
D	973	$^4I_{15/2} \rightarrow {}^4I_{11/2}$	$^4I_{11/2} \rightarrow {}^4F_{7/2}$	ESA	[19, 20]
E	842	-	$^4I_{13/2} \rightarrow {}^4S_{3/2}$	PA	[21]
F	808	-	$^4I_{11/2} \rightarrow {}^4F_{3/2}$	PA	[22]
G	794	$^4I_{15/2} \rightarrow {}^4I_{9/2}$	$^4I_{13/2} \rightarrow (^2H(2),^4G)_{11/2}$	ESA	-
H	713	-	$^4I_{13/2} \rightarrow {}^4F_{7/2}$	PA	-
I	691	-	$^4I_{11/2} \rightarrow {}^4F_{9/2}$	PA	[23, 24]
J	642	$^4I_{15/2} \rightarrow (^4F,^4I)_{9/2}$ -	$^4I_{13/2} \rightarrow {}^4F_{5/2}$	ESA PA	[25, 26]
K	577	-	$^4I_{11/2} \rightarrow {}^4G_{9/2}$	PA	[24, 27]
L	558	-	$^4I_{11/2} \rightarrow (^4G,^2G(2))_{7/2}$	PA	-
M	546	$^4I_{15/2} \rightarrow {}^4S_{3/2}$	$^4I_{13/2} \rightarrow {}^4F_{9/2}$	ESA	-
N	501	-	$^4I_{13/2} \rightarrow (^4G,^2H(2))_{11/2}$	PA	-
O	480	- $^4I_{15/2} \rightarrow {}^4F_{7/2}$	$^4I_{13/2} \rightarrow {}^4G_{9/2}$	PA ESA	-
P	465	-	$^4I_{13/2} \rightarrow (^4G,^2G(2))_{7/2}$ $^4I_{11/2} \rightarrow {}^2P_{3/2}$	PA	-
R	430	-	$^4I_{11/2} \rightarrow {}^4G_{5/2}$	PA	-
S	418	-	$^4I_{11/2} \rightarrow (^4G,^2G(1))_{7/2}$	PA	-
T	399	-	$^4I_{11/2} \rightarrow {}^2P_{3/2}$	PA	-

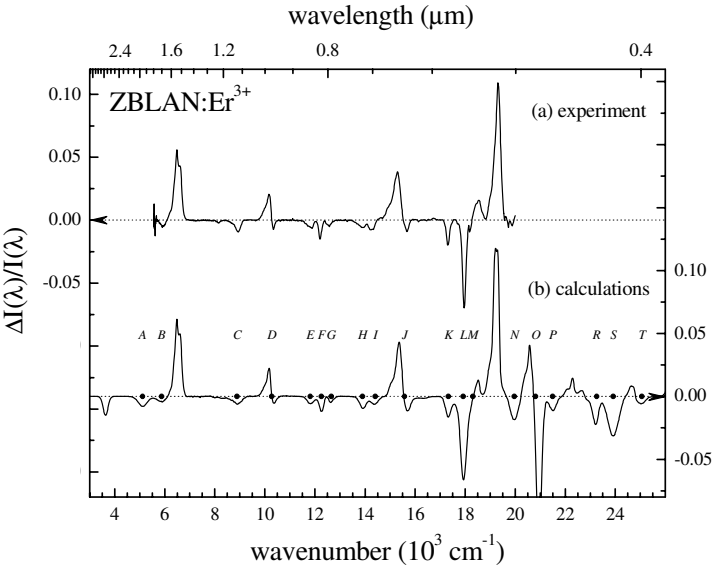

Fig.1. Experimental (a) and simulated (b) EST spectra together with proposed anti-Stokes emission excitation wavelengths (•)

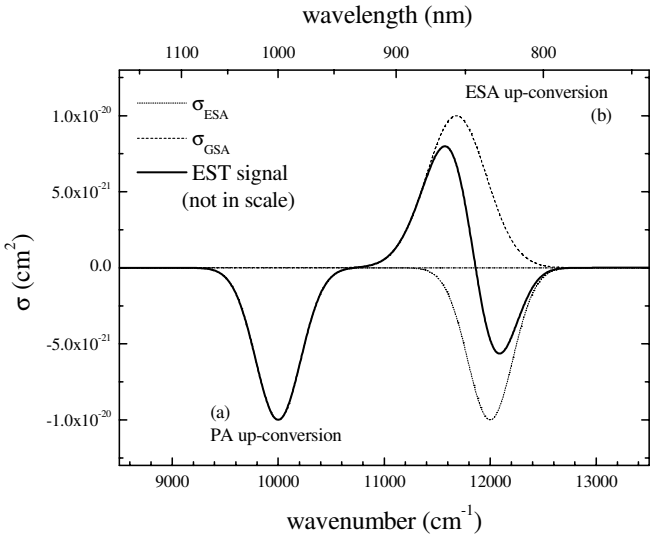

Fig.2. Theoretical EST spectrum and relationships between GSA and ESA transitions.